Magnetic fluctuations of a large nonuniform plasma column

J. E. Maggs[a] and G. J. Morales
Physics and Astronomy Department, University of California, Los Angeles, Los Angeles, California 90095

(Received 17 December 2002; accepted 13 March 2003)

A broad experimental survey is made of the properties of spontaneously generated magnetic fluctuations in a large linear device in which the plasma density has different cross-field gradient scales. It includes steep gradients at the plasma–wall edge as well as at an interior plasma–plasma interface, thus phenomena of interest to magnetic fusion research as well as to space plasma physics is illustrated. Fluctuations in uniformly magnetized columns and plasmas with an axial gradient in the confining magnetic field are studied. Some of the highlights include the identification of a universal spectrum for drift-Alfvén turbulence and the role of partial reflections in shaping the spectra. © *2003 American Institute of Physics.* [DOI: 10.1063/1.1572814]

I. INTRODUCTION

The properties of spontaneously generated magnetic fluctuations are a topic of considerable interest to several areas of contemporary plasma research. These fluctuations have been predicted to enhance electron heat transport[1–3] in toroidal confinement devices and under certain conditions a turbulent spectrum of magnetic fluctuations can generate dynamo-currents.[4–6] Active control of spontaneous magnetic fluctuations has been recently demonstrated to improve plasma confinement[7] in reversed field pinches. In naturally occurring plasmas such as the Earth's auroral ionosphere and the solar corona, a large level of magnetic fluctuations is present in regions where field-aligned energetic electrons are generated[8] and also where transverse acceleration of various ion species occurs.[9] Large amplitude magnetic fluctuations are also considered to contribute to structure formation in astrophysical plasmas.[10]

The generation of magnetic fluctuations in a strongly magnetized plasma is ultimately related to modulations of field-aligned currents. The modulations are often driven by the free energy associated with gradients in the ambient plasma parameters such as the density, temperature, zero-order current and confinement magnetic field. Because of the inherent anisotropic response of a plasma in the presence of a strong confinement field, the magnetic fluctuations of interest are primarily shear Alfvén waves modified by gradient effects. Of course, mode transformation to compressional Alfvén waves can play an important role, particularly when steep gradients and/or boundaries are present.[11]

Since shear Alfvén waves do not propagate for frequencies above the ion gyrofrequency Ω_i, the spectrum of spontaneous magnetic fluctuations characteristically spans a frequency band $\Omega_i > \omega > \pi v_A/L$, where v_A represents the Alfvén speed and L is the largest scale length of the system. An important aspect in the study of spontaneously generated magnetic fluctuations is the shape of their frequency spectrum. In particular, it is of interest to determine the relative importance of coherent and broad band components and how the various spectral features change over a broad range of plasma conditions. At a level of greater detail, it is also of interest to identify the spatial structure and polarization of the vector components of the magnetic fluctuations. To obtain such information under controlled conditions it is necessary to make detailed measurements inside large plasmas capable of supporting Alfvénic fluctuations. This is the essence of the present study.

This experimental survey aims to identify the characteristic features of spontaneously generated magnetic fluctuations in a magnetized, large plasma column under reproducible conditions. It should be mentioned that an analogous study in the environment of a research tokamak has been previously reported and the results have been related to toroidal physics effects.[12] The present investigation emphasizes the behavior that results when the plasma contains several gradient scales and a self-consistent, field-aligned current system is present.

The experiments described in this manuscript are performed in the upgraded Large Plasma Device (LAPD-U) operated by the Basic Plasma Science Facility (BASPF) at the University of California, Los Angeles (UCLA). Since plasmas in this device are generated by thermionic emission and subsequent acceleration of electrons from a cathode, it is possible to obtain plasma columns that display internal, cross-field gradients in addition to the usual edge gradients in contact with the walls. The internal gradients are simply generated by having regions of the cathode with different emissivity. In the present configuration this cathode imprinting was achieved by bombardment of the cathode with energetic ions along selected field lines for an extended period of time.

Steep internal gradients can arise in fusion devices under enhanced confinement conditions [e.g., H-modes (Refs. 13, 14)] and have recently been the focus of attention in studies of the auroral ionosphere. For instance, observations made by the POLAR spacecraft[8] traveling through the plasma-sheet boundary layer (where steep density gradients are present) have shown that large amplitude Alfvén waves of short transverse-scale are embedded within large-scale magnetic fluctuations. The significance of the phenomenon is that

[a]Electronic mail: maggs@physics.ucla.edu

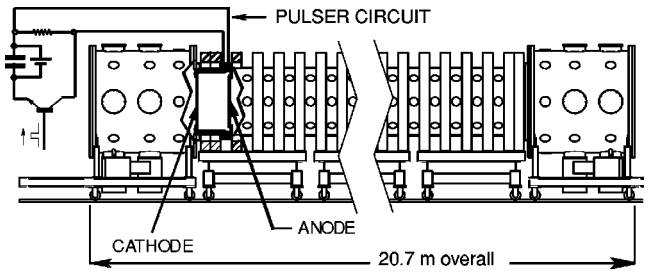

FIG. 1. A truncated schematic of the LAPD-U showing some of the vacuum chamber and axial field magnets, a cutaway of the source region, and the discharge pulser circuit.

these events have been temporally and spatially correlated with the generation of auroral beams.

In addition to investigating the properties of the magnetic fluctuations in the various transverse gradient regions, the present study explores the dependencies on axial machine length over a factor of 2 and on the strength of the uniform magnetic field, also over a factor of 2. The modification of the fluctuations in a plasma with an axial gradient in the confinement magnetic field is also considered.

The major results obtained are: (1) Amplitude levels of low frequency (below f_{ci}) magnetic fluctuations decrease with increasing axial magnetic field; (2) Cross-field gradients are characterized by low frequency magnetic noise: Drift-Alfvén waves in regions of steep gradient, and evanescent Alfvén waves in gentler gradient regions; (3) Spectra of steep-gradient driven magnetic fluctuations are characterized by a universal $\exp(-\alpha\omega)$ frequency behavior; (4) In terms of absolute amplitudes, the largest magnetic signals correspond to the lowest frequencies generated in gentle gradients; (5) Statistical behavior of edge magnetic fluctuations is Gaussian; (6) In the presence of an axial field gradient the spontaneous magnetic fluctuations are quenched for frequencies above the local ion cyclotron frequency; (7) The axial gradient causes the edge fluctuations to behave as if the plasma had a shorter effective length and an effective lower magnetic field.

The manuscript is organized as follows. Section II describes the properties of the apparatus used and the measurement techniques. Section III presents the major experimental findings including the behavior in a uniform magnetic field (Sec. III A), and the effect of a magnetic field gradient (Sec. III B). A discussion of the results and their connection to previous work is found in Sec. IV. Conclusions and suggestions for follow-up studies are presented in Sec. V.

II. APPARATUS AND TECHNIQUES

The experimental results presented in Sec. III are obtained in plasmas generated in the upgraded Large Plasma Device (LAPD-U) operated by the Basic Plasma Science Facility at UCLA. A schematic of the device is shown in Fig. 1. A magnetized plasma column of adjustable axial extent is generated by primary electrons emitted from a cathode. The cathode consists of a radiatively heated nickel plate that is coated with barium oxide, but the emission characteristics of the surface are sensitive to the conditioning of the plate. In the present study the plate has been previously subjected to bombardment by energetic aluminum ions (~ 2 keV) over an extended period along magnetic field lines that cover approximately one-half of the emission area. This imprinting of the cathode essentially results in the juxtaposition of two plasma columns that exhibit an internal density gradient in addition to the usual edge gradients in contact with the walls of the surrounding vacuum vessel. The diameter of the plasma column is approximately 60 cm and is determined primarily by the size of the coating on the plate.

The primary electrons are accelerated by a potential difference of 45 V applied on a pulsed basis to a semitransparent copper mesh (transmission efficiency $\sim 50\%$) located a distance of 55 cm from the cathode. This mesh acts as the effective anode for the device since all other surfaces in contact with the plasma are floating. In the present studies the injected currents range from 8 to 10 kA. The accelerated primaries drift into a vacuum chamber, whose overall axial extent is 19.35 m, and strike neutral He gas at a fill pressure of $1-2\times10^{-4}$ Torr to generate a He^+ plasma with a greater than 50% degree of ionization. This is the main experimental region in which the measurements reported are made. In this region the maximum density of the plasmas generated are in the range of $2-3\times10^{12}$ cm^{-3}, while the electron temperature is approximately 8 eV with the ion temperature in the range of 1 eV. The experimental measurements reported are made in the current-free region beyond the anode to which the previously stated parameters apply. The current-carrying plasma between the cathode and anode is likely to display slightly different parameter values, which at this stage can not be measured. It should further be noted that waves can propagate between the cathode–anode region and the main plasma column with the anode mesh acting as a partially transmitting boundary analogous to the partially reflecting mirrors used in lasers.

In the present studies the typical pulse length applied to the anode is in the range of 8–12 ms with a repetition rate of 1 Hz. The measurements reported here are taken in the nearly steady-state portion of the discharge 2 ms before the termination of the discharge pulse. To ensure a high degree of repeatability in the starting time of the discharge, a steady (dc) current is maintained by 40 V across 50 Ω between anode and cathode. This current maintains a weak discharge which provides for easy breakdown of the neutral gas when the main discharge pulse is applied.

The plasma column is confined radially by an axial magnetic field, B_0, generated under CW conditions by an 18 m-long solenoid formed from a total of 90 water-cooled coils. The coils are grouped in carts which are individually fed by a regulated power supply having a 0.1% ripple. The total available power that can be delivered to the solenoid is 4 MW, which can generate confinement fields up to 4 kG on a limited operational basis. In the present study we use two different magnetic field configurations. One is the standard uniform magnetic field operation. For the results reported in Sec. III A, a range of uniform B_0 from 700 to 1300 G is explored. The other configuration investigated corresponds to a confinement field having a constant axial gradient. This is accomplished by adjusting the current feeding individual

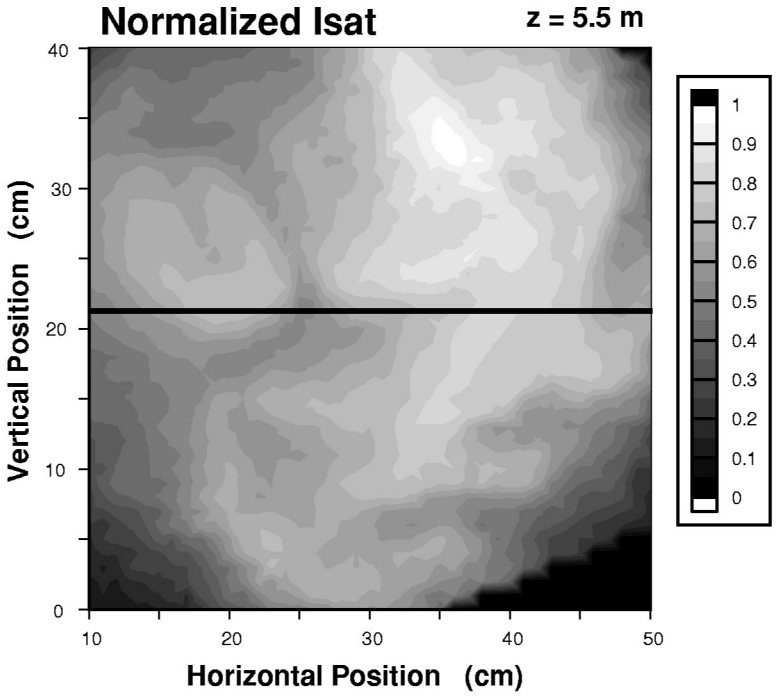

FIG. 2. Gray-scale contours of ion saturation current in a plane (y,x) perpendicular to the confinement magnetic field at a distance $z=5.5$ m from the cathode for steady-state conditions at 1000 G and 8.5 kA. The plasma profile results from the juxtaposition of two columns generated from regions of the cathode having different emissivity. This plasma generation method creates an "interior gradient" region in the vicinity of $20<x<25$ (cm) along the black horizontal line. The data presented in later figures are taken along this line.

carts so that a constant drop between the fields at the center of adjacent carts is obtained. The results reported in Sec. III B correspond to a gradient magnetic field with a maximum field of 1600 G in the anode region, decreasing to a level of 400 G in the last cart at the opposite end of the machine. Regardless of the magnetic configuration used, the magnetic field strength in the cathode–anode region decreases steadily toward the cathode surface due to end-flaring in the last magnet cart. The field at the cathode is a factor of 0.67 smaller than that at the anode, a value determined by the distance between heater and cathode.

Within the time window over which the data is taken, the plasma is in a steady-state condition in which the global values of the temperature and plasma density are nearly constant in time. In this regime the mean free-path of the background electrons is a few centimeters. The electron distribution is a Maxwellian with a temperature limited by classical heat conduction (due to Coulomb collisions) to the open ends of the device. The heating power is provided by the collisional slowing down of the primary electrons. This heating power is independent of magnetic field or machine length. The plasma density is nearly constant because of the large axial extent of the plasma column. That is, the plasma is inertially confined with losses at the ends of the device occurring at the ion sound speed. During this stage the small density loses at the ends are balanced by partial ionization provided by the background electrons and the primaries. When the primary current is terminated the electron temperature decreases rapidly with a time scale of about 100 μs, while the density decays very slowly with a time scale of about 10 ms. Densities in excess of 10^{11} cm^{-3} are present as long as 50 ms after the discharge current is shut-off.

In the present study plasma columns having 10 and 18 m are examined. The nominal column length at 18 m is simply determined by the length of the solenoid. In this arrangement the uncompensated magnetic field in the magnet cart farthest from the cathode gives rise to flaring field lines that bring plasma in contact with a large end chamber. The 10-m column is achieved by rotating a hinged aluminum plate across the magnetic field at an axial distance roughly midway along the total length of the vacuum chamber. In this case the plasma is terminated in good electrical contact with the floating plate. It should be mentioned that the choice of 10 m corresponds to the earlier version[15] of the LAPD device in which we have previously performed studies of magnetic fluctuations generated by microscopic density[16] and temperature filaments.[17]

The experimental results described in Sec. III are obtained from small magnetic probes (i.e., B-dot loops) inserted into the plasma through ports located at different axial positions in the equatorial plane of the machine. The probes are connected to computer controlled shafts that permit the recording of data at selected positions within the cross section of the plasma. Typically the frequency spectra investigated are averaged over 20 plasma pulses at each spatial location, thus they should be properly described as the ensemble averaged spectra. Two different probes are used in the broad survey reported. Both consist of mutually perpendicular loops capable of measuring the simultaneous evolution of the 3-components of the magnetic field fluctuations. One probe is larger ($\sim$8 mm) than the other ($\sim$4 mm), thus they have different sensitivity. Whenever spectra are compared (as in Sec. III) data obtained with the same probe are used to eliminate variations unrelated to the plasma behavior. The frequency range of the fluctuations investigated here is well separated from the characteristic resonant frequencies of each probe.

Figure 2 is a gray-scale shaded contour plot of the ion saturation current taken near the end of the plasma discharge during steady-state conditions obtained for $B_0=1000$ G at an

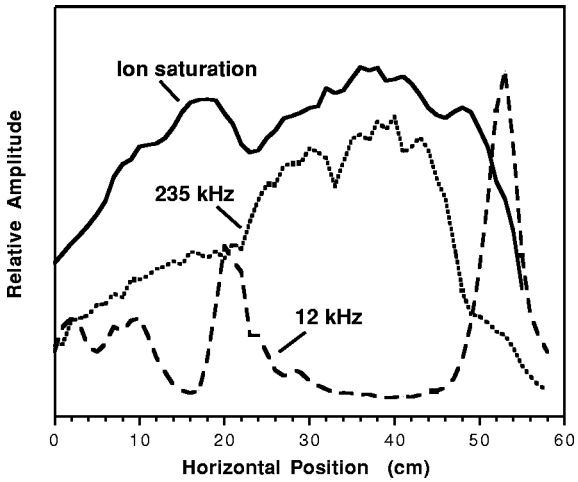

FIG. 3. Spatial dependence along the horizontal x-direction of the ion saturation current (top solid curve). In the regime of operation the ion saturation current essentially represents the plasma density. For comparison, the spatial behavior of the prominent spectral peaks at 12 kHz (dashed curve) and 235 kHz (dotted curve) identified later in Fig. 4 are also shown. The linear scales for each curve are adjusted to facilitate visualization.

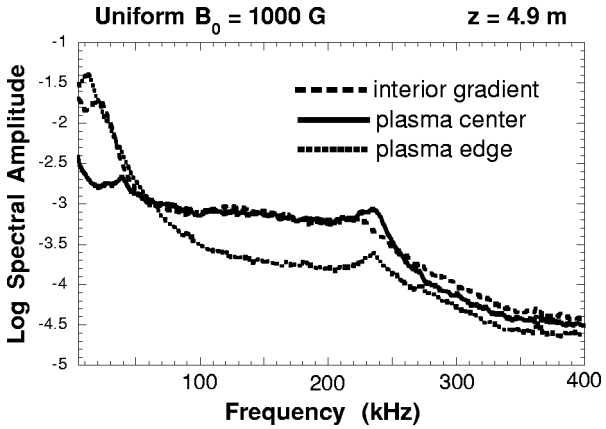

FIG. 4. Frequency spectra (log scale) of the amplitude of the transverse component of the spontaneous magnetic fluctuations at an axial position $z=4.9$ m from the cathode for three different horizontal positions x along the black line in Fig. 2. The spectrum at the "plasma edge" (dotted curve) corresponds to $x=53$ cm, the "interior gradient" (dashed curve) to $x=22$ cm, and the "plasma center" (solid curve) to $x=39$ cm. The uniform confinement field is 1000 G and the column length is 18 m.

axial position $z=5.5$ m from the cathode. Since, for the present conditions, the electron temperature has weak variation across the column, the ion saturation current contours essentially represent the plasma density profile. It is seen that the plasma consists of two columns generated by the two different emitting regions of the cathode. A larger one is located within horizontal positions $30<x<50$ cm and vertical positions $10<y<40$ cm, while the smaller one is at $10<x<25$ cm, $20<y<30$ cm. The juxtaposition of these columns results in a plasma having a relatively steep "interior gradient region" in the vicinity of $20<x<25$ cm along the horizontal black line. Profile data, presented in subsequent figures, are taken along this cut across the plasma column.

The solid black curve near the top of Fig. 3 corresponds to the ion saturation current along the cut shown in Fig. 2. It shows a "plasma center region" with relatively weak gradient between horizontal positions $x=24$ and $x=50$ cm. To the right of the center there is a steep "plasma edge" with a maximum gradient around $x=53$ cm. To the left of the center there is also a region having a steep gradient but of opposite sign located near $x=22$ cm. This is the "interior gradient" region, far from conducting walls. Far to the left, near $x=0$ cm is the other plasma edge, but now having a gentle gradient. In subsequent figures the comparative properties of magnetic fluctuations in the center, rightmost plasma edge, and the interior gradient are explored. The dotted and dashed curves in Fig. 3 present information to be described later in Sec. III A.

III. EXPERIMENTAL RESULTS

A. Uniform magnetic field

This subsection describes the properties of the spontaneous magnetic fluctuations observed in plasma columns confined by a uniform magnetic field.

Figure 4 displays the measured frequency spectra of magnetic fluctuations in the three different spatial regions identified in Sec. II, i.e., the plasma edge ($x=53$ cm), the plasma center ($x=39$), and the interior gradient ($x=22$ cm) along the reference cut shown in Fig. 2. The vertical axis corresponds to the log (base 10) of the amplitude of the transverse component $(B_x^2+B_y^2)^{1/2}$ of magnetic fluctuations at a given frequency. The horizontal scale covers a frequency range extending slightly above the ion cyclotron frequency ($f_{ci}=380$ kHz). The strength of the confinement field is 1000 G and the discharge current is 8 kA. The axial position of the measurements is $z=4.9$ m from the cathode for a plasma column having a length of 18 m. The amplitude of the parallel component of the fluctuations is not displayed because they are found to be so small that they are within the alignment errors of the probe. These magnetic fluctuations are essentially of shear polarization.

It is seen in Fig. 4 that the plasma edge (dotted curve) and interior gradient (dashed curve) exhibit enhanced fluctuations at frequencies below 50 kHz, while the plasma center (solid curve) does not. This low-frequency band is associated with drift-Alfvén waves at frequencies typically below a tenth of the ion cyclotron frequency (i.e., $f/f_{ci}<0.1$) which are driven unstable by the steep, cross-field gradients in plasma pressure. The spectra in the three different regions show broad band shear-wave noise extending up to a spectral peak feature at about 235 kHz, a value which is significantly below f_{ci} for the He^+ plasma column having 1000 G uniform field.

The spatial structure of the prominent spectral peaks identified in the spectra of Fig. 4 is illustrated by the dotted and dashed curves previously encountered in Fig. 3. It is now useful to relate their behavior to the density profile represented by the solid curve in the top portion of the figure. Note that this figure uses a linear scale that is arbitrarily selected for each mode since the focus is on their spatial structure. It is seen from Fig. 3 that the low frequency peak at 12 kHz (dashed curve) is significantly enhanced in the

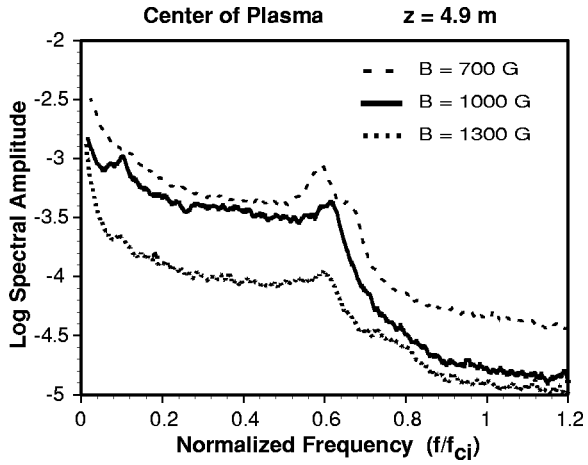

FIG. 5. Scaling of frequency spectra (log scale) at the center of the plasma with strength of the uniform confinement field B_0 over the range of 700–1300 G. The frequency f is normalized to the ion cyclotron frequency f_{ci} to test for universality. The shape of the spectra does not change with B_0, but the absolute level of the fluctuations exhibits a favorable decrease with increasing B_0. $z=4.9$ m and $x=39$ cm.

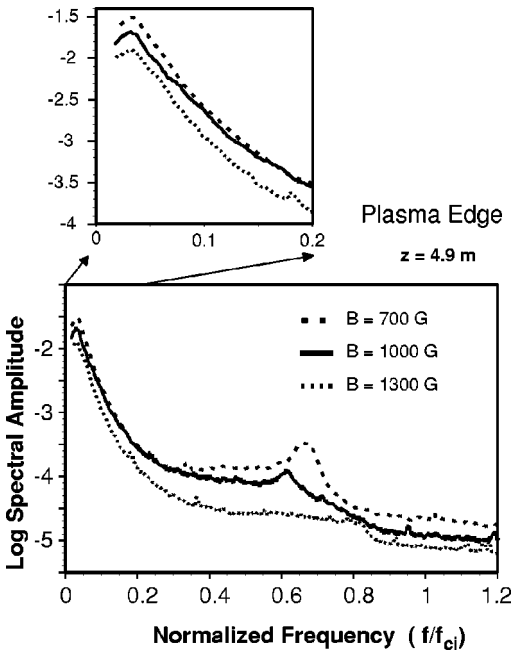

FIG. 6. Scaling of frequency spectra (log scale) at the plasma edge with strength of the uniform confinement field B_0 over the range of 700–1300 G, as in Fig. 5. In this spatial region the shape of the spectrum for frequencies below 0.25 f_{ci} is invariant and displays an exponential tail, but the details of the spectral shape vary at the higher frequencies. The decrease in fluctuation amplitude with increasing B_0 is also found at the plasma edge.

regions of steep gradients and is of very low amplitude in the plasma center where the gradient is mild. A modest enhancement is also seen near the gentle edge gradient in the region, $0<x<10$ cm. In contrast to the localized behavior of the low frequency fluctuations, the spectral peak at 235 kHz (dotted curve) exhibits a global mode structure. The peak amplitude of this mode coincides with the ''plasma center'' and the related eigenfunction broadly follows the average density profile. A similar trend has also been observed in the Tokopole II tokamak (as seen in Fig. 4 of Ref. 12). This behavior suggests a useful complementary technique to assess the density profile of a plasma based on magnetic fluctuations; the locations of steep gradients are marked by the low frequency noise while the average behavior follows the global eigenmode.

The dependence of the spectra of magnetic fluctuations at the plasma center on the strength of the confining magnetic field is shown in Fig. 5 for $B_0=700$, 1000, and 1300 G. The vertical scale is the log of the amplitude as in Fig. 4, but now the horizontal frequency axis is scaled to the ion cyclotron frequency in order to identify scaling trends. The axial location is $z=4.9$ m, as in Fig. 4. Figure 5 shows that the shape of the spectra of magnetic fluctuations at the plasma center is essentially independent of magnetic field strength. The spectra consist of broad band shear Alfvén wave noise extending up to a prominent peak at $\sim 0.6\, f_{ci}$. For frequencies above this value the shear wave noise is strongly suppressed. The low frequency limit is masked by the spectral features associated with the spatially decaying noise generated at the distant steep gradient regions, as exemplified by the behavior of the 12 kHz signal in Fig. 3. A splitting of the $0.6\, f_{ci}$ peak is found to develop at 700 G (dashed curve). The magnitude of the split is roughly $0.1\, f_{ci}$. Another important feature shown in Fig. 5 is that the level of the magnetic fluctuations across the entire band up to f_{ci} exhibits a very favorable decrease as the strength of the confinement magnetic field is increased. The amplitude of the broad band fluctuations drops roughly by a factor of 10 as the field is increased by a factor of 2, for a fractional change, $\delta B/B_0$, of 20.

The behavior at the steep plasma edge ($x=53$ cm) is shown in Fig. 6 for the same conditions as in Fig. 5. In the edge region the low frequency ($f<0.2\, f_{ci}$) component of the spectrum exhibits a universal scaling, but not the high frequency component. However, the decrease in fluctuation level for larger confinement fields occurs for all frequencies. The inset at the top of the figure shows the behavior of the spectrum associated with the drift-Alfvén fluctuations driven by the gradient in pressure. It consists of a broad peak centered around $0.05\, f_{ci}$ followed by an exponential tail. The value of the exponential decay rate is independent of the magnetic field strength. The nature of the exponential tail is masked by broad band noise for frequencies above $0.2\, f_{ci}$. The prominent eigenmode peak at $0.6\, f_{ci}$ is clearly visible for 1000 G (solid curve), as is consistent with the global eigenmode shown in Fig. 3. However, for 700 G (dashed curve) it is found that the peak is shifted to higher frequency. In fact, this peak corresponds to the right-hand side of the split peak identified at the plasma center in Fig. 5. It appears that the eigenmode of the lower-frequency component of the split peak found at the center does not reach the edge at $x=53$ cm.

Figure 7 provides a comparison of the spectra of magnetic field fluctuations at the plasma edge, in contact with metallic walls (top panel), to that generated within the interior gradient (bottom panel), surrounded by plasma. The quantity displayed is the log of the fluctuation amplitude for different values of the confinement field, as in Figs. 5 and 6.

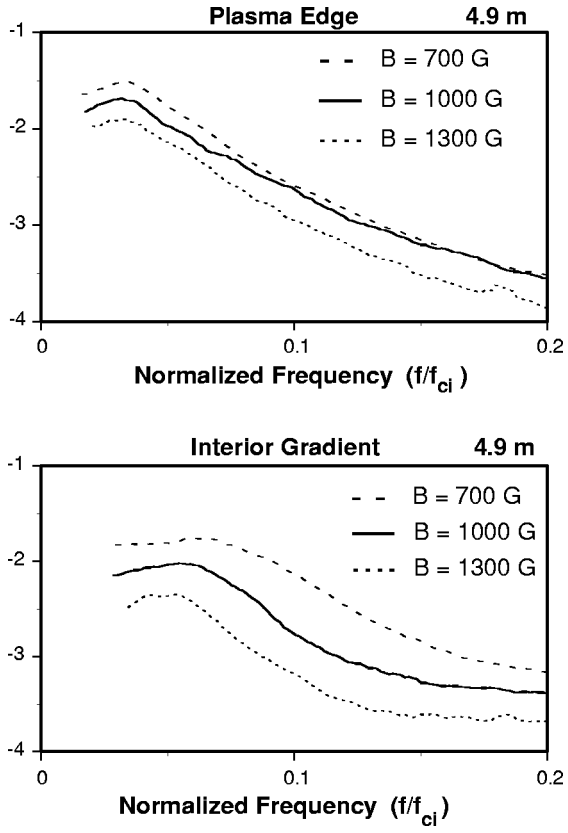

FIG. 7. Comparison of the spectra of magnetic field fluctuations at the plasma edge, in contact with metallic walls (top panel), to that generated within the interior gradient (bottom panel), surrounded by plasma. B_0 is varied from 700 to 1300 G, $z=4.9$ m.

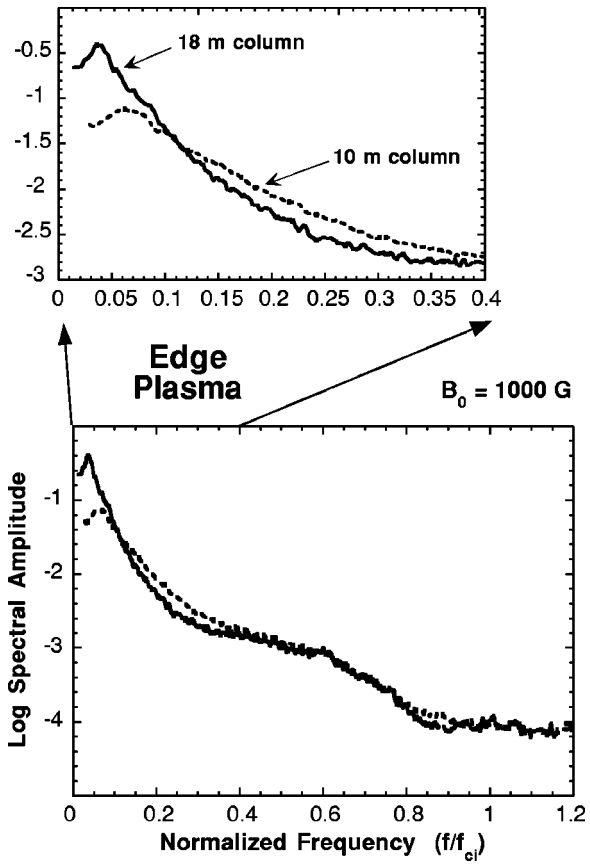

FIG. 8. Dependence of frequency spectra (log scale) at the plasma edge on the axial length of the plasma column. The solid curve is for 18 m column and the dotted curve is for 10 m. The spectra above 0.2 f_{ci} is insensitive to column length. The top insert presents an expanded view of the lower frequency band. It shows a small shift toward lower frequencies for the longer column, as is expected for axially standing drift-Alfvén modes. $z=8.75$ m, $x=53$ cm, and $B_0=1000$ G.

The characteristic exponential tail of the spectra is seen to prevail for the interior gradient and the decay rate is also independent of magnetic field. The interior gradient spectra, however, is more severely masked by the broad band noise of the surrounding plasma. Also, the peak of the fluctuations seems to be shifted to lower frequency at the plasma edge in comparison to that at the interior gradient.

The dependence of the fluctuation spectra at the plasma edge ($x=53$ cm) on the length of the plasma column is shown in Fig. 8 for $B_0=1000$ G at $z=8.75$ m. The solid curve corresponds to 18 m, and the dotted curve to 10 m, as explained in Sec. II. It is found that the spectra differ only at frequencies below 0.2 f_{ci}. As is clear from the insert at the top, the spectral peak at low frequencies occurs at a lower frequency for the longer machine. This behavior is consistent with a drift-Alfvén wave whose frequency is determined by the parallel wavelength set by the machine length. It is also seen that the characteristic exponential decay, identified in Fig. 7, exists for the long and short machines. However, the value of the decay constant increases for the longer plasma. The amplitude of the spectral peak also increases.

The effect of plasma column length on the spectra at the plasma center ($x=39$ cm) is shown in Fig. 9 for $B_0=1000$ G, at $z=8.75$ m. As in Fig. 7, the solid curve corresponds to 18 m and the dotted one to 10 m. The remarkable finding is that the spectra are virtually identical in shape and in amplitude, which is not the case at the plasma edge. Due to this behavior, the display in Fig. 9 has now been changed to a linear scale in order to resolve the small changes that do occur. In this linear scale the strong suppression of the broad band shear wave noise above 0.65 f_{ci} becomes quite pronounced. The suppression effect is independent of the length of the plasma column, and is a phenomenon that has been shown in Fig. 5 to exhibit a universal dependence on the strength of the confinement magnetic field. In addition, the spectra of magnetic fluctuations at the plasma center are not only insensitive to machine length, but their shape is essentially the same at significantly different axial positions along the plasma column.

It is seen in Fig. 9 that, in the shorter column, the amplitude of the noise below 0.6 f_{ci} is enhanced by about 30%. There is also some evidence that sharper peaks embedded within a continuum begin to appear. Both trends are consistent with modes being partially reflected from the conducting plate that terminates the 10 m column, as described in Sec. II. In the longer column, however, the peak is seen to broaden and increase in amplitude, again by roughly 30%.

B. Gradient in the magnetic field

This subsection examines the spontaneous magnetic fluctuations of a plasma in which the confinement field has

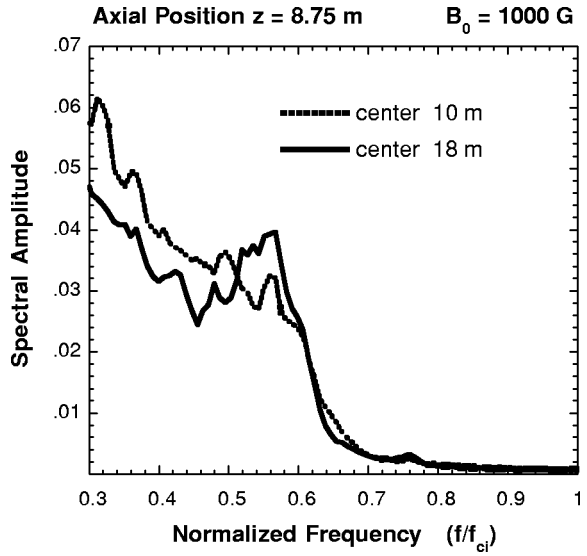

FIG. 9. Frequency spectra at the plasma center for plasma columns having axial length of 10 and 18 m, using the same convention of Fig. 8. Note that a linear scale is used here to identify the relatively small changes. It is seen that in the center the spectral amplitude is independent (within 30%) of column length. It consists of continuous shear Alfvén wave noise that is strongly suppressed above the frequency of the global mode close to $0.6\,f_{ci}$. $z=8.75$ m, $x=39$ cm, and $B_0=1000$ G.

an axial gradient. In the case presented next, the high-field region is on the cathode side of the device where the discharge current is injected. We refer to this configuration as ''decreasing magnetic field.'' The technique used for achieving this condition is explained in Sec. II. An important effect in this case is that the frequency below which shear Alfvén waves can propagate [i.e., $f<f_{ci}(z)$] decreases with distance, z, from the anode towards the far end of the machine. This implies that the extended plasma imposes a natural low-pass filter on the magnetic noise at each axial position.

Figure 10 displays the spectra of magnetic fluctuations

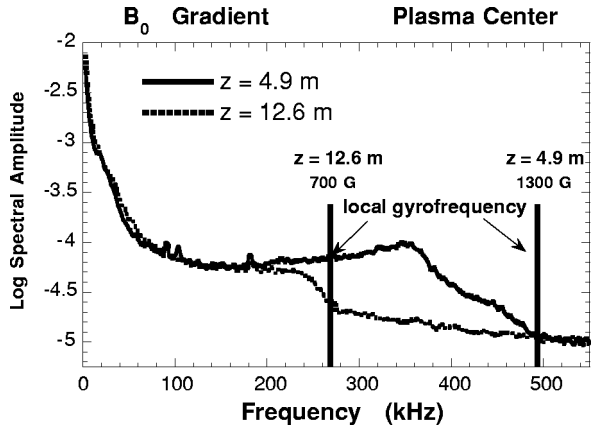

FIG. 10. Frequency spectra (log scale) at the plasma center in the presence of a piecewise-linear axial gradient in the confinement magnetic field. The magnetic field is 1600 G at the cathode and 400 G at the end of the device 18 m away. The solid curve is at axial location $z=4.9$ m ($B_0=1300$ G) from the cathode and the dotted curve is at $z=12.6$ m ($B_0=700$ G). The local value of the gyrofrequency at these positions is indicated by the vertical lines. These curves are to be compared to the uniform B_0 counterparts shown in Fig. 5.

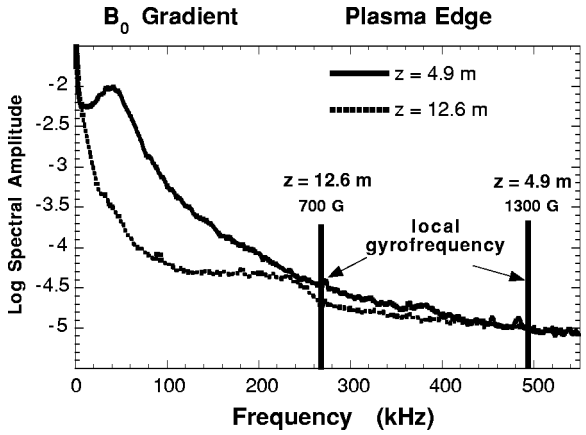

FIG. 11. Frequency spectra (log scale) at the plasma edge ($x=56$ cm) in the presence of a linear axial gradient in the confinement magnetic field, as in Fig. 10.

(log scale) measured at the plasma center for two different axial positions. At $z=4.9$ m (solid curve) the local value of the magnetic field is 1300 G and at $z=12.6$ m (dotted curve) it is 700 G. The local value of the ion gyrofrequency is indicated by the vertical lines.

There are several important effects illustrated by Fig. 10. One is the clear evidence that the spontaneous magnetic fluctuations are quenched for frequencies above the local ion cyclotron frequency. This conclusively demonstrates that the fluctuations are propagating shear Alfvén waves. The fact that the waves in the frequency band between the two vertical lines are quenched in going from $z=4.9$ to 12.6 m indicates that the noise has its origin in the cathode–anode region of the plasma where parallel currents are injected. The broad band of excited waves propagate down the plasma column and are selectively filtered as they approach the local cyclotron frequency.

Figure 11 displays the behavior of the edge spectra (at $x=53$) in the presence of an axial field gradient. For higher frequencies ($f>2\times10^5$ Hz) the phenomena sampled is the same as in the plasma center, i.e., shear wave noise is naturally filtered by the gradient. However, the lower frequencies associated with unstable drift-Alfvén waves behave differently. At the larger axial position, where the field is weaker, the low frequency noise at a given x position decreases significantly and the prominent low-frequency peak disappears.

To obtain a better understanding of the results shown in Fig. 11, a comparison is made with the spectra measured in a uniform plasma but with a field strength, $B_0=1300$ G, equal to the local value prevailing at $z=4.9$ m in the presence of the axial gradient. The comparison is shown in Fig. 12. Since, in the presence of an axial gradient, the edge plasma naturally flares out, it is more appropriate to compare results that exhibit equivalent phenomena. In this case the comparison is made at a horizontal position, x, where the low frequency peak achieves its maximum value. This corresponds to $x=53$ cm for the uniform case (solid curve) and to $x=56$ cm for the axial gradient (dotted curve). It is now clear that the radial position (x location) is shifted to larger values and the frequency of the peak is also shifted to a higher value

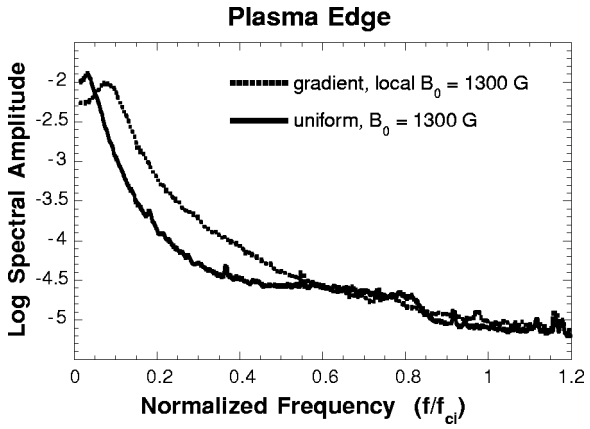

FIG. 12. Comparison of spectra (log scale) at the plasma edge for a plasma with uniform magnetic field (solid curve) and another with the axial field gradient described in Sec. II (dotted curve). The horizontal position, x, for each is chosen to correspond to where the low frequency peak is largest ($x=53$ cm for the uniform case and $x=56$ cm for the gradient) at the same axial position $z=4.9$ m. Comparison with Figs. 7 and 8 suggests that the gradient results in an effectively shorter plasma with lower magnetic field.

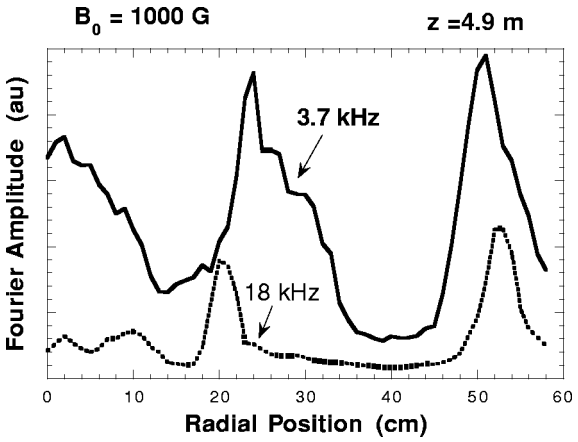

FIG. 14. The profiles of the spectral amplitude of low frequency noise are shown for two frequencies, 3.7 kHz (solid curve) and 18 kHz (dashed curve). The noise at 18 kHz corresponds to drift-Alfvén waves driven by steep gradients and is therefore spatially localized. The noise at 3.7 kHz corresponds to evanescent shear Alfvén waves driven by gentle gradients. These waves have a much broader spatial distribution.

in the presence of the gradient. A frequency shift of this type is shown in Fig. 8 to be associated, for a uniform field, with a change in column length. The shorter column results in a peak having higher frequency. The enhancement in the total amount of fluctuation power in the presence of the gradient is also consistent with the dependence on magnetic field strength shown in Fig. 7 for a uniform field. For lower magnetic fields the fluctuation power over the entire band increases. The picture that emerges from these comparisons is that the axial gradient causes the edge fluctuations to behave as if the plasma had a shorter effective length and an effective lower magnetic field, while the flaring field lines increase the radial location of the peak.

Figure 13 displays the effect of the axial gradient on the spatial dependence of the prominent peaks shown in Fig. 4 for a uniform field at the same axial position, $z=4.9$ m. The

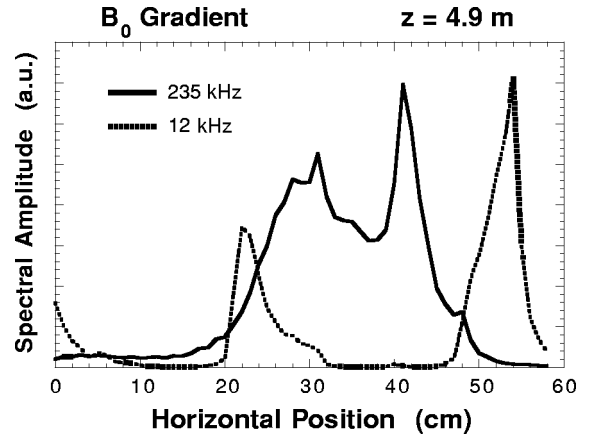

FIG. 13. Spatial dependence along the horizontal x-direction of the prominent spectral peaks (linear scale) at 12 kHz (dotted curve) and 235 kHz (solid curve) shown in Fig. 4 for a uniform magnetic field. Here a magnetic field gradient is present, as described in Sec. II. The amplitude scale is chosen to help visualization. Using the low frequency peaks as an indicator of steep gradients, it is found that the higher-frequency mode is confined to the central region of the plasma. Axial position is $z=4.9$ m.

235 kHz peak is represented by the solid curve and the 12 kHz by the dotted curve. The scale of the linear amplitude for each signal is chosen to help visualization. Using the location of the peak of the low frequency signal to identify the steep-gradient regions, it is found that the higher frequency mode exhibits a larger degree of localization to the plasma center than its counterpart for the uniform field case.

C. Very-low frequencies

In most of the figures previously discussed the spectral range $f<0.03\,f_{ci}$ has been omitted. This interval corresponds to very-low frequency phenomena that can not be identified as propagating shear Alfvén waves since the associated wavelengths do not fit within the axial length of the device (18 m). Magnetic fluctuations, however, are observed at these very low frequencies, but they must be interpreted as evanescent fields associated with oscillatory currents of finite extent. The primary driver for such currents may have an intrinsic electrostatic character, but it should not be concluded that the associated magnetic signals are small. In fact, it is found that for a uniform field $B_0=1000$ G magnetic signals below 5 kHz exist over the extended gentle-gradient regions of the plasma. The amplitude of the signals is a factor of 100 larger than those of the broad band shear-wave noise that coexists in these regions.

To provide a better perspective of the location of the very-low frequency fluctuations, Fig. 14 presents the spatial dependence of the fluctuation amplitude at 3.7 kHz (solid curve) together with that of drift-Alfvén modes at 18 kHz (dashed curve) for $B_0=1000$ G. It should be noted that the drift-Alfvén mode is driven by the steep gradients and thus remains spatially localized, while the low frequency signals are driven in regions where the pressure gradient is gentle (i.e., small diamagnetic drift). To probe the detailed properties and dependencies of the very-low frequency signals, plasma pulse-lengths much longer than are used in this investigation are required.

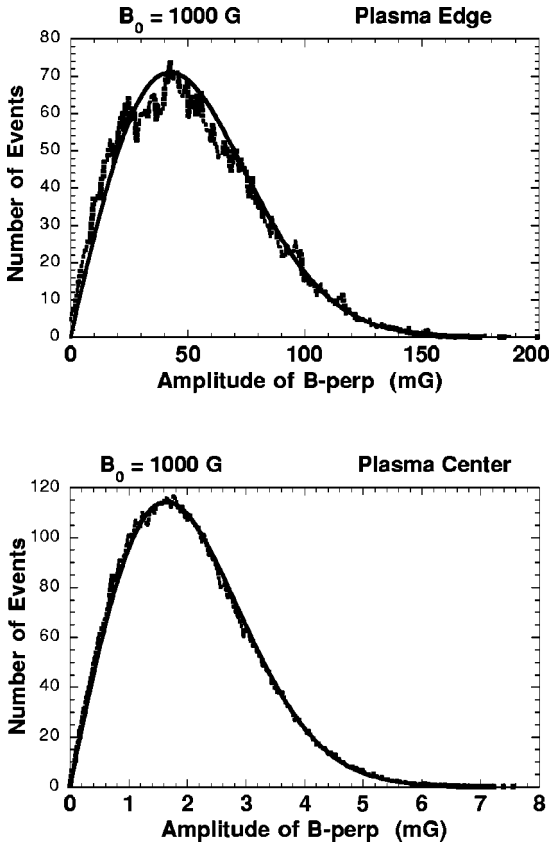

FIG. 15. Statistical properties of spontaneous magnetic field fluctuations observed under various conditions. Top: plasma edge at $B_0=1000$ G, bottom: plasma center at $B_0=1000$ G. The solid curve is a fitted Gaussian distribution and the dotted curve is data.

D. Statistics of fluctuations

A statistical analysis of the individual time traces used to generate the ensemble average spectra is shown in Fig. 15 which shows the number of times (events) in a fixed time interval the wave form has a particular amplitude. The magnetic field is uniform with a value of 1000 G. The top panel pertains to the steep plasma edge and the bottom panel to the plasma center. The field amplitude corresponds to $(B_x^2+B_y^2)^{1/2}$ which is intrinsically two-dimensional, hence the peak is shifted away from zero.

The solid curves shown in the two panels correspond to Gaussian functions whose parameters are suitably adjusted. The close agreement obtained demonstrates that the source of fluctuations at the plasma center and at the plasma edge obeys ''Gaussian statistics.'' It is to be emphasized that the fluctuations at the plasma center to which this property applies are the broad band shear modes above $0.05\,f_{ci}$ since a high-pass filter has been used that eliminates the very-low frequencies.

Broad band shear waves have typical fluctuation amplitudes that are about a factor of 20 smaller than those of the edge drift-Alfvén modes. From the absolute calibration provided in Fig. 15 it is seen that the broad band noise has a fractional fluctuation level of $\delta B/B_0\approx 2\times 10^{-6}$ while the gradient-driven modes achieve a typical level of $\delta B/B_0\approx 5\times 10^{-5}$. Perhaps the lowest threshold condition for the emergence of nonlinearity in the behavior of shear Alfvén waves is that the fractional level of magnetic fluctuations is comparable to the electron-ion mass ratio, i.e., $\delta B/B_0\sim$ m/M. At this level the distortion due to finite wave amplitude becomes comparable to linear dispersive effects. For these experiments this level corresponds to $\delta B/B_0\sim 10^{-4}$. Using this criteria as a gauge of nonlinearity, gradient-driven fluctuations are near the nonlinear regime while the broad band fluctuations are likely to be in the linear regime.

IV. DISCUSSION

In this section an assessment is presented of the factual information extracted from the broad survey previously described. Connections to other studies are indicated where possible.

It has been documented that the magnetic fluctuations associated with steep plasma pressure gradients exhibit properties characteristic of drift-Alfvén modes that are highly localized to the gradient region. It is found that these modes can exist at the interface between a plasma and a conducting wall (edge plasma) as well as at an interior plasma–plasma interface. While the edge plasma behavior is intrinsic to magnetic confinement fusion devices, the plasma–plasma interface arises naturally in space plasmas, an example being the plasma–sheet boundary layer. The features and scaling identified in the present study provide guidance for the interpretation of magnetic signals observed in these widely different environments. It is deduced from the present study that it is natural for the fluctuations generated at interior plasma–plasma interfaces to consist of two embedded transverse scales. The short scale is associated with drift-Alfvén modes while the long scale arises from evanescent fields generated in the neighboring gentle-gradient regions. Embedding of Alfvénic fluctuations has been observed in the Polar spacecraft[8] and possibly also in the Tokopole II tokamak.[12]

A feature that appears to be substantiated by the present survey is that the frequency spectra of drift-Alfvén turbulence exhibits a universal shape. It consists of a broad lower-frequency peak in the interval of $0.05<f/f_{ci}<0.1$ and it is followed by an exponentially decreasing tail [i.e., $S(\omega)\sim\exp(-\alpha\omega)$] that eventually connects at higher frequencies to the shear-wave broadband noise. The decay constant α is insensitive to the value of the magnetic field but shows a variation with axial length. The universality of the spectra has been previously suggested[18] by our independent studies in an earlier linear device in which such turbulence has been generated in density striations[16] and temperature filaments.[17]

The exponential frequency spectra has been also observed in the Continuous Current Tokamak (CCT) (as seen in Fig. 1 of Ref. 19) under quite different conditions from those in the linear machine used in the present study. Thus, the behavior documented here seems to be broader in scope. It is to be noted that the frequency spectra reported in the Tokapole II investigation[12] does not show a definitive trend, since the features are found to vary with position and with toroidal safety factor q. However, for the larger q-values the log–log plots (see Figs. 10, 11, and 12 in Ref. 12) exhibit different

power-law dependencies in different frequency bands. Such dependencies are characteristic of an exponential spectrum when displayed in a log–log format.

The decrease in the amplitude of the fluctuations as the magnetic field is increased is found to be nonlinear, with the fractional fluctuation $\delta B/B_0$ of the broadband noise decreasing by a factor of 20 as B_0 increases by a factor of 2. In the present study the increases in B_0 essentially correspond to a lowering of the electron beta. An analogous decrease has also been reported in the Tokapole II study but there the trend has been surmised to be regulated by the value of q, or equivalently the plasma current. It is likely that in the present study the plasma current is also partly responsible for the broad band shear wave fluctuations but the relevant parameter is the ratio of the effective electron drift velocity v_D to the Alfvén speed v_A. Of course, in a linear device this ratio can also be related to an effective safety factor $q_L=(B_0/B_p)(2\pi a/L)$, where B_p is the poloidal field, a is the plasma radius, and L is the length of the current carrying column. The relationship admits a simple interpretation, namely, $q_L=(4\pi\delta_i/L)v_A/v_D$, where δ_i is the ion skin-depth.

The observation of a sharp spectral peak near $0.6\,f_{ci}$ accompanied by an apparent quenching of the broad band noise over a frequency interval that is well separated from f_{ci} (e.g., Fig. 9) is very puzzling and its origin has received much scrutiny on our part. We considered a variety of known mechanisms, that failed to provide a satisfactory explanation of the features associated with this phenomenon. We mention, for the record, three obvious candidates. One is the presence of a minority ion species resulting in an ion–ion hybrid resonance. The most likely candidate mass for this effect is lithium since it would yield a resonant frequency at $0.58\,f_{ci}$. However, measurements with a mass analyzer give no trace of such a species being present and no known sources in the machine would yield this element.

Another plausible mechanism, previously invoked by researchers[20] investigating the behavior of launched Alfvén waves in high-density plasma, is ion-neutral collisions. Evaluation of the relevant dispersion relation for the parameters of the LAPD-U device indicates that the frequency interval over which such effects play a role are confined to $0.9\,f_{ci}<f<f_{ci}$. Thus this mechanism can be ruled out.

Another interesting mechanism that could play a role in suppressing noise below f_{ci} is the coupling of the spontaneously generated shear Alfvén waves to Paoloni modes.[21] These modes are compressional Alfvén waves with mode number $m=+1$ that can propagate at frequencies below f_{ci} in bounded plasma columns in which a relatively tenuous region exists between the core plasma and the surrounding vacuum vessel. The mechanism has been previously claimed[20] to explain the damping of launched shear modes in a frequency band that is consistent with the suppression region observed in our experiment. However, we have searched for modes with compressional polarization in the band above $0.65\,f_{ci}$ and have not been able to obtain conclusive evidence that this mechanism is present in our studies.

It has been pointed out by Leneman[22] that the observed invariance of the spectral peak to changes in magnetic field strength (e.g., Fig. 5) implies that the axial wavelength of this mode, assuming it belongs to the shear mode branch, is constant. In fact, for the parameters of relevance this wavelength corresponds to approximately twice the distance between the cathode and the partially reflecting mesh anode. This insight, when complemented by the behavior deduced from the spatial dependence of the spectra in the presence an axial magnetic field gradient (e.g., Fig. 10) provides a clue to the underlying process.

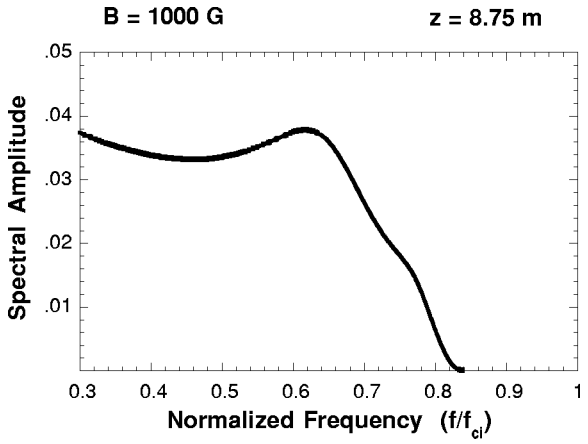

FIG. 16. Predicted spectral amplitude at axial location $z=8.75$ m for $B_0=1000$ G in the main plasma column. The model consists of partial wave reflections between cathode and anode where the average magnetic field is smaller than in the main column. To be compared to Fig. 9.

The picture that emerges is that plasma currents, either associated with the fast primary electrons in the source region or return currents in the main plasma column, give rise to the excitation of shear modes. These modes in turn experience multiple reflections between the cathode and the anode and a fraction of the wave power (as in a laser cavity with a partially reflecting mirror) propagates out into the large plasma column.

The additional element contributing to the quenching of the noise above $0.65\,f_{ci}$ is that the strength of the confining magnetic field decreases from the anode toward the cathode. In essence, in this region the wave propagation is akin to that depicted in Fig. 10, but in the opposite spatial direction. The higher frequency modes reflected from the anode are filtered out as they approach the cathode while those at the lower frequencies reach the cathode, are reflected and return to the large plasma column giving rise to the observed spectra.

Figure 16 provides a quantitative example of the behavior expected from the resonant cavity model. This figure displays the predicted spectral amplitude at axial position $z=8.75$ m for $B_0=1000$ G, as is appropriate for the data of Fig. 9. In the calculation leading to Fig. 16 the plasma parameters are selected to provide the closest resemblance to the observed behavior. One of the parameters is the mean value of the magnetic field in the cathode–anode region. This can be deduced from the vacuum-field code used to design the magnet system. Another parameter is the wave reflection coefficient of the anode R_A, which is taken as 0.2. The calculation includes electron–ion Coulomb collisions and ion–neutral collisions in the evaluation of the local dispersion relation of shear Alfvén waves in the source and

main plasma regions. This yields the parallel wave numbers k_s in the source region, and k_p in the main plasma, for transverse wave number $k_\perp = \pi/a$, where a is the plasma radius.

The quantity plotted in Fig. 16 is $|\psi|$ where

$$\psi(z,\omega) = \exp\{i[k_s(\omega)L_s + k_p(\omega)z]\}/\{1 - R_A \exp[2ik_s(\omega)L_s]\},$$

represents the scaled fluctuating field at frequency ω and L_s is the distance between the cathode and the anode.

It is seen from Fig. 16 that the spectrum predicted by the model exhibits a peak close to the observed value, and a strong quenching above $0.8\, f_{ci}$, also consistent with the behavior shown in Fig. 9. The rightmost shoulder feature in Fig. 16 corresponds to the second resonant mode between the anode and cathode; its prominence is sensitive to ion damping. From the strong similarity seen between the predictions of the model and the observed phenomena, it is suggestive that the fundamental elements of the model are the correct explanation for the puzzling spectral properties. Of course, a more detailed calculation is required to reproduce the finer features as well as the absolute amplitude level of the fluctuations.

It is worth noting that the physics associated with the build-up of partially reflecting shear Alfvén waves, as apparently occurs spontaneously in the cathode-anode region, forms the basis of some models[23,24] proposed to explain the formation of auroral arcs. In such an environment the lower ionosphere plays a role analogous to the partially reflecting anode.

V. CONCLUSIONS

A broad experimental survey has been made of the properties of spontaneously generated magnetic fluctuations in a large linear device in which the plasma density has different cross-field gradient scales. It includes steep gradients at the plasma–wall edge as well as at an interior plasma–plasma interface, thus phenomena of interest to magnetic fusion research as well as to space plasma physics is illustrated. The plasma configuration also has a self-consistent current system that in the main plasma column resembles the conditions of the auroral ionosphere. The dependencies of the fluctuations on system length (10 and 18 m) and strength of the uniform confining field (700–1300 G) have been investigated. The modifications of the fluctuations produced by a confining magnetic field with an axial gradient (ranging from 1600 G to 400 G) has been illustrated.

The major observational results are: (1) Amplitude levels of low frequency (below f_{ci}) magnetic fluctuations decrease with increasing axial magnetic field; (2) Cross-field gradients are characterized by low frequency magnetic noise: Drift-Alfvén waves in regions of steep gradient, and evanescent Alfvén waves in gentler gradient regions; (3) Spectra of steep-gradient driven magnetic fluctuations is characterized by a universal $\exp(-\alpha\omega)$ frequency behavior; (4) In terms of absolute amplitudes, the largest magnetic signals correspond to the lowest frequencies generated in gentle gradients; (5) Statistical behavior of gradient-driven magnetic fluctuations is Gaussian; (6) In the presence of an axial field gradient the spontaneous magnetic fluctuations are quenched for frequencies above the local ion cyclotron frequency; (7) The axial gradient causes the edge fluctuations to behave as if the plasma had a shorter effective length and an effective lower magnetic field.

A comparative study of the results with various models has brought out that partial reflection of shear Alfvén by a conducting boundary can play a major role in shaping the observed spectra. Since phenomena of this type can be present in various naturally occurring plasmas as well as in magnetic confinement devices, a future focused study on this subject appears to be highly desirable.

ACKNOWLEDGMENTS

The authors thank Dr. D. Leneman for his incisive comments concerning the role of the cathode–anode region and M. VanZeeland for providing a magnetic probe of small dimension.

This work is sponsored by the NSF and ONR. The experiment was performed in the Basic Plasma Science Facility (BAPSF) operated at UCLA under joint sponsorship of the NSF and DOE.

[1] J. D. Callen, Phys. Rev. Lett. **39**, 1540 (1977).
[2] A. B. Rechester and M. N. Rosenbluth, Phys. Rev. Lett. **40**, 38 (1978).
[3] T. Ohkawa, Phys. Lett. A **67**, 35 (1978).
[4] U. Frisch, A. Pouquet, J. Leorat, and A. Mazure, J. Fluid Mech. **68**, 769 (1975).
[5] S. Ortolani and D. D. Schnack, *Magnetoydrodynamics of Plasma Relaxation* (World Scientific, Singapore, 1993).
[6] S. C. Praeger, Plasma Phys. Controlled Fusion **41**, A129 (1999).
[7] T. Bolzonella, P. Martin, S. Martini, L. Marelli, R. Pasqualotto, and D. Terranova, Phys. Rev. Lett. **87**, 195001 (2001).
[8] J. R. Wygant, A. Keiling, C. A. Cattell, M. Johnson, R. L. Lysak, M. Temerin, F. S. Mozer, C. A. Kletzing, J. D. Scudder, W. Peterson, C. T. Russell, G. Parks, M. Brittnacher, G. Germany, and J. Spahn, J. Geophys. Res. **106**, 18675 (2000).
[9] I. Roth and M. Temerin, Astrophys. J. **477**, 940 (1997).
[10] D. R. Goncalves, L. V. Jatenco-Pereira, and R. Opher, Astrophys. J. **501**, 797 (1998).
[11] A. Hasegawa, J. Geophys. Res. **81**, 5083 (1976).
[12] D. E. Graessle, S. C. Praeger, and R. N. Dexter, Phys. Fluids B **3**, 2626 (1991).
[13] F. Wagner, G. Becker, K. Behringer, D. Campbell, A. Eberhagen, W. Engelhardt, G. Fussmann, O. Gehre, J. Gerhardt, G. v. Gierke, G. Hass, M. Huang, F. Karger, M. Keilhacker, O. Klüber, M. Kornherr, K. Lackner, G. Lisitano, G. C. Lister, H. M. Mayer, D. Meisel, E. R. Müller, H. Murman, H. Niedermeyer, W. Poschenrieder, H. Rapp, H. Röhr, F. Schneider, G. Siller, E. Speth, A. Stäbler, K. H. Steurer, G. Venus, O. Vollmer, and Z. Yü, Phys. Rev. Lett. **49**, 1408 (1982).
[14] R. J. Taylor, M. L. Brown, B. D. Fried, H. Grote, J. R. Liberati, G. J. Morales, and P. Pribyl, Phys. Rev. Lett. **63**, 2365 (1989).
[15] W. Gekelman, H. Pfister, Z. Lucky, D. Leneman, and J. Maggs, Rev. Sci. Instrum. **62**, 2875 (1991).
[16] J. E. Maggs and G. J. Morales, Phys. Plasmas **4**, 290 (1997).
[17] A. T. Burke, J. E. Maggs, and G. J. Morales, Phys. Plasmas **7**, 1397 (2000).
[18] G. J. Morales, J. E. Maggs, A. T. Burke, and J. R. Peñano, Plasma Phys. Controlled Fusion **41**, A519 (1999).
[19] G. Fiksel, S. C. Praeger, P. Pribyl, R. J. Taylor, and G. R. Tynan, Phys. Rev. Lett. **75**, 3866 (1995).
[20] Y. Amagishi and M. Tanaka, Phys. Rev. Lett. **71**, 360 (1993).
[21] F. J. Paoloni, Phys. Fluids **18**, 640 (1975).
[22] D. Leneman (private communication, October 2002).
[23] C. K. Goertz and R. W. Boswell, J. Geophys. Res. **84**, 7239 (1979).
[24] G. Haerendel, *High Latitude Space Plasma Physics*, edited by B. Hultqvist and T. Hagfors (Plenum, New York, 1983), p. 515.